

Instability of a spatially developing liquid sheet

By LUIGI DE LUCA AND MICHELA COSTA

Università degli Studi di Napoli ‘Federico II’ – DETEC, P.le Tecchio, 80, Napoli 80125, Italy

(Received 27 June 1995 and in revised form 13 August 1996)

The linear stability of an inviscid two-dimensional liquid sheet falling under gravity in a still gas is studied by analysing the asymptotic behaviour of a localized perturbation (wave-packet solution to the initial value problem). Unlike previous papers the effect of gravity is fully taken into account by introducing a slow length scale which allows the flow to be considered slightly non-parallel. A multiple-scale approach is developed and the dispersion relations for both the sinuous and varicose disturbances are obtained to the zeroth-order approximation. These exhibit a local character as they involve a local Weber number We_η . For sinuous disturbances a critical We_η equal to unity is found below which the sheet is locally absolutely unstable (with algebraic growth of disturbances) and above which it is locally convectively unstable. The transition from absolute to convective instability occurs at a critical location along the vertical direction where the flow Weber number equals the dimensionless sheet thickness. This critical distance, as measured from the nozzle exit section, increases with decreasing the flow Weber number, and hence, for instance, the liquid flow rate per unit length. If the region of absolute instability is relatively small it may be argued that the system behaves as a globally stable one. Beyond a critical size the flow receptivity is enhanced and self-sustained unstable global modes should arise. This agrees with the experimental evidence that the sheet breaks up as the flow rate is reduced. It is conjectured that liquid viscosity may act to remove the algebraic growth, but the time after which this occurs could be not sufficient to avoid possible nonlinear phenomena appearing and breaking up the sheet.

1. Introduction

Thin liquid sheet (or curtain) flows have been extensively studied because of their theoretical and technological interest. The variety of applications, ranging from the disintegration of liquid sheets in the atomization context to the coating process, is well summarized in Finnicum, Weinstein & Ruschak (1993), whereas Chubb *et al.* (1994) analysed the possible space application of sheet flows as low-mass radiating surfaces.

Both the interface shape and the stability of liquid sheets have been investigated in prior papers. As first pointed out by Squire (1953), the sheet break-up results from the growth of transverse waves, having lines of crests orthogonal to the streamwise direction. Two kinds of waves are possible at any given frequency: either the two free surfaces of the sheet are both displaced in the same direction to form sinuous waves, or they move in opposite directions, as in the varicose waves. Squire (1953) and later Hagerty & Shea (1955) performed an inviscid analysis on a sheet of uniform thickness and found that instability occurs if the Weber number (ratio of inertia forces to liquid surface tension) is greater than unity. Brown (1961) carried out an experimental investigation on the behaviour of a liquid curtain impinging on a rapidly moving surface. He found the minimum liquid flow rate to maintain a stable curtain by

observing that equilibrium must be maintained at a free edge between the inertia forces and the surface tension σ . When a free edge appears because of the formation of a hole, such a hole does not grow if the oncoming momentum flux is greater than 2σ ; otherwise it grows and the curtain disintegrates.

Subsequent papers took into account the effects of liquid viscosity. Crapper, Dombrowski and Jepson (1975*b*) demonstrated that viscosity has no effect on the initial stages of wave growth. Lin (1981) asserted that viscosity has the dual roles of increasing both the amplification rate and the damping rate of the disturbances. This result was then confirmed by Lin, Lian & Creighton (1990) who found that, contrary to the case of a round jet (Lin & Lian 1989), the critical Weber number is insensitive to the gas-to-liquid density ratio and the Reynolds number. Li & Tankin (1991) showed that the liquid viscosity introduces an additional temporal mode which destabilizes a certain range of wavenumbers and is referred to as viscosity-enhanced instability.

One of the main weaknesses in the past studies is that little attention was devoted to the analysis of the *absolute* or *convective* character of the instability. In fact some authors did try to explain the disagreement between the experimental data and the results of the classical *temporal* modes analysis by supposing a growth of disturbances in space rather than in time (*spatial* modes analysis). Crapper, Dombrowski & Pyott (1975*a*) observed that if photographs were taken at different times, the wave amplitude was unchanged at the same distance from the nozzle exit section; Lin (1981) used Gaster's theorem to derive the amplification rate in space from the growth rate in time.

The spatial modes approach would indicate if a perturbation introduced at a certain point in space amplifies or not away from that point. However, solutions of the dispersion relation with complex wavenumbers α (having imaginary part $\alpha_i < 0$) and real frequencies ω do not necessarily represent convective instabilities, as emphasized by Drazin & Reid (1981), who stressed how 'naive use of spatial modes may indicate that a stable flow is unstable'. Indeed, the actual physical nature of the disturbance can be interpreted only by resorting to a study of the behaviour in time and space of a wave-packet solution to the initial-value problem. In other words, one has to verify if spatial modes emerge as time tends to infinity on solutions of the initial value problem. These concepts were well clarified in the context of plasma physics by Clemmow & Dougherty (1969), who also gave some practical suggestions for diagnosing the nature of the instability. Briefly, they expressed solutions of initial-value problems in the form of Fourier integrals, and showed that if the real α -axis may be smoothly transformed into a line which is a map of the real ω -axis, then the spatial modes correctly indicate stability or instability. The ideas of Clemmow & Dougherty (1969) are proposed in the present paper as an alternative approach to study the impulse response of the system. The approach to the initial-value problem, qualified below, due to Briggs (1964) and Bers (1975), was extended to several fluid flows instabilities by Chomaz, Huerre & Redekopp (1988), Huerre & Monkewitz (1990), and Monkewitz (1990).

In the light of the preceding discussion some of the previous papers concerned with the stability of liquid sheets have to be revisited in order to better discuss the occurrence and the actual character of the instability. In the present paper the instability of a two-dimensional liquid sheet is studied within an inviscid approximation. In fact, it is known that for the sheet flow regimes of practical interest and vertical distances (from the nozzle exit section) greater than just a few nozzle widths, the sheet flow strictly agrees with that predicted by the very simple inviscid inertia-gravity model (e.g. de Luca & Costa 1995). The role of viscosity will be further discussed later in the paper, when discussing the results.

Unlike all the previous papers, the effect of gravity, i.e. non-uniform sheet thickness,

is taken into account. The vertical variation of thickness breaks the Galilean invariance along the streamwise direction, i.e. the flow in its unperturbed state is spatially developing. However, the evolution length scale of the basic flow is large with respect to the curtain thickness and a slow length scale S can be introduced (slightly non-parallel flow). This multiple-scale approach leads one to consider that the basic flow quantities, as well as amplitude and wavenumber of disturbances, change over the slow length scale. As a consequence, the dispersion relation between wavenumber and frequency (obtained by solving the boundary value problem to the lowest order) exhibits a local character and the flow stability properties that are established, refer to local velocity and curtain thickness.

The analysis is performed within the linear theory, which is believed to yield a reliable understanding of the physical mechanism governing the instability onset before sheet disintegration.

2. Problem formulation

Consider a Newtonian incompressible liquid of density ρ_l emanating from a nozzle (slit) of infinite length and falling under gravity through a still gas of density ρ_g (figure 1). Both liquid and gas motions are supposed to be inviscid. Let (x, y, z) be a Cartesian coordinate system with the positive z -axis in the direction of the gravitational acceleration. The sheet dynamics is investigated by means of the linear hydrodynamic stability theory and the problem consists of determining the liquid velocity potential $\phi(x, y, z, t)$ (defined as $\nabla\phi = -V$, V being the liquid velocity) and the gas velocity potential $\psi(x, y, z, t)$ satisfying Laplace's equation in the two media (t is the time variable). The closure is given by enforcement of the kinematic condition of no flow through the interface and the dynamic condition expressing the pressure jump at the interface as a function of the surface tension. The perturbed interface position is $\eta(x, z, t)$.

Introducing the following dimensionless variables:

$$x = \frac{x^*}{b}, \quad y = \frac{y^*}{b}, \quad z = \frac{z^*}{b}, \quad t = \frac{t^* \bar{U}}{b},$$

$$\phi = \frac{\phi^*}{\bar{U}b}, \quad \psi = \frac{\psi^*}{\bar{U}b}, \quad \eta = \frac{\eta^*}{b}, \quad R = \frac{R^*}{b},$$

where an asterisk denotes dimensional quantities, \bar{U} is the mean velocity at the slit exit section, b is the slit half-width and $1/R$ is the curvature of the interface, the equations to be solved are

$$\nabla^2 \phi = 0, \tag{1}$$

$$\nabla^2 \psi = 0, \tag{2}$$

$$\frac{\partial \eta}{\partial t} - \nabla \phi \cdot \nabla \eta + \frac{\partial \phi}{\partial y} = 0, \quad y = \pm \eta, \tag{3}$$

$$\frac{\partial \eta}{\partial t} - \nabla \psi \cdot \nabla \eta + \frac{\partial \psi}{\partial y} = 0, \quad y = \pm \eta, \tag{4}$$

$$\frac{1}{2}(\nabla \phi)^2 - \frac{1}{2}r(\nabla \psi)^2 - \frac{bgz}{\bar{U}^2}(1-r) - \frac{\partial \phi}{\partial t} + r \frac{\partial \psi}{\partial t} - \frac{1}{2} = \frac{1}{WeR}, \quad y = \pm \eta, \tag{5}$$

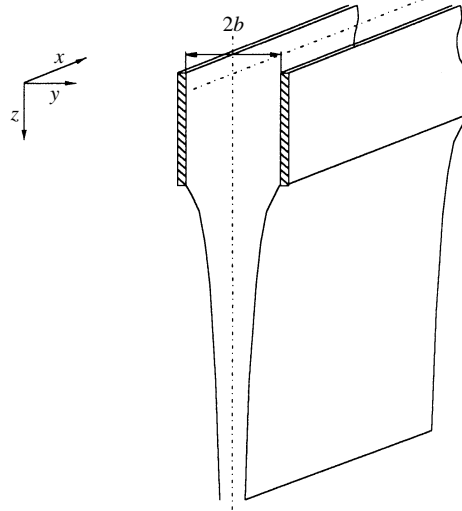


FIGURE 1. Schematic representation of the liquid sheet.

where g is the gravitational acceleration, r is the ratio of the gas-to-liquid density and the flow Weber number is

$$We = \rho_l \bar{U}^2 b / \sigma, \quad (6)$$

being σ the surface tension and

$$\frac{1}{R} = \nabla \cdot \left(\frac{\nabla \eta}{[1 + (\nabla \eta)^2]^{1/2}} \right) \quad (7)$$

the curvature.

The perturbed flow variables are taken to have the form

$$\phi = \bar{\phi} + \phi', \quad (8)$$

$$\psi = \bar{\psi} + \psi', \quad (9)$$

$$\eta = \bar{\eta} + \eta', \quad (10)$$

namely they are divided into a steady mean flow and an unsteady disturbance which is supposed to be small. By substituting (8)–(10) into (1)–(5), neglecting the perturbation quadratic terms and expanding both the mean and fluctuation quantities in a Taylor series about the unperturbed interface position (so as to apply the boundary conditions (3)–(5) at $y = \pm \bar{\eta}$), the basic flow and disturbances equations are derived. The unperturbed state of the liquid is inferred from

$$\nabla^2 \bar{\phi} = 0, \quad (11)$$

$$\frac{\partial \bar{\phi}}{\partial y} - \nabla \bar{\phi} \cdot \nabla \bar{\eta} = 0, \quad y = \pm \bar{\eta}, \quad (12)$$

$$\frac{1}{2} (\nabla \bar{\phi})^2 - \frac{1}{2} \frac{bgz}{\bar{U}^2} (1-r) = \frac{1}{We R}, \quad y = \pm \bar{\eta}. \quad (13)$$

The disturbance equations are

$$\nabla^2 \phi' = 0, \quad (14)$$

$$\nabla^2 \psi' = 0, \quad (15)$$

$$\frac{\partial \eta'}{\partial t} - \nabla \phi' \cdot \nabla \bar{\eta} - \nabla \bar{\phi} \cdot \nabla \eta' - \eta' \frac{\partial}{\partial y} (\nabla \bar{\phi}) \cdot \nabla \bar{\eta} + \frac{\partial \phi'}{\partial y} + \eta' \frac{\partial^2 \bar{\phi}}{\partial y^2} = 0, \quad y = \pm \bar{\eta}, \quad (16)$$

$$\frac{\partial \eta'}{\partial t} - \nabla \psi' \cdot \nabla \bar{\eta} + \frac{\partial \psi'}{\partial y} = 0, \quad y = \pm \bar{\eta}, \quad (17)$$

$$\frac{\eta'}{2} \frac{\partial}{\partial y} [(\nabla \bar{\phi})^2] + \nabla \bar{\phi} \cdot \nabla \phi' - \frac{\partial \phi'}{\partial t} + r \frac{\partial \psi'}{\partial t} = \frac{1}{We R'}, \quad y = \pm \bar{\eta}. \quad (18)$$

Owing to the gravity, the basic flow variables are not invariant under continuous translations along the z -coordinate, i.e. the basic flow is not parallel, but spatially developing. However, if the flow varies slowly along z , use can be made of the multiple-scale method. Accordingly the slow length scale $Z = \epsilon z$ is introduced, where ϵ is a small dimensionless parameter characterizing the non-parallelism of the flow, and the fluctuation quantities are defined as follows:

$$\phi'(x, y, Z, t) = [\phi_0(y, Z) + \epsilon \phi_1(y, Z) + \dots] e^{-i\omega t + i\beta x + i\gamma(Z)/\epsilon}, \quad (19)$$

$$\psi'(x, y, Z, t) = [\psi_0(y, Z) + \epsilon \psi_1(y, Z) + \dots] e^{-i\omega t + i\beta x + i\gamma(Z)/\epsilon}, \quad (20)$$

$$\eta'(x, Z, t) = [\eta_0(Z) + \epsilon \eta_1(Z) + \dots] e^{-i\omega t + i\beta x + i\gamma(Z)/\epsilon}, \quad (21)$$

where ω and β are dimensionless frequency and wavenumber (along the x -direction) respectively.

Equations (19)–(21) also contain a WKB approximation for the exponential term. The parameter ϵ is assumed to be the curtain slenderness ratio, namely the ratio of the slit half-width to a typical vertical length S :

$$\epsilon = \frac{b}{S} = \frac{2gb}{U^2}. \quad (22)$$

2.1. Basic flow

The unperturbed flow being symmetric with respect to the (x, z) -plane, the study is limited to the half of the physical domain between the symmetry plane and the free surface. The basic velocity potential $\bar{\phi}(y, Z)$ and boundary shape $\bar{\eta}(Z)$ are evaluated as asymptotic power series of ϵ :

$$\bar{\phi}(y, Z) = \sum_{j=0}^{\infty} \epsilon^j \bar{\phi}_j(y, Z), \quad (23)$$

$$\bar{\eta}(Z) = \sum_{j=0}^{\infty} \epsilon^j \bar{\eta}_j(Z). \quad (24)$$

It is convenient to normalize the basic velocity potential with respect to S (instead of b) and to introduce the following variable (e.g. Geer 1977):

$$\bar{\Phi}(y, Z) = \epsilon \bar{\phi}(y, Z) \quad (25)$$

such that

$$\bar{\Phi}(y, Z) = \sum_{j=0}^{\infty} \epsilon^j \bar{\Phi}_j(y, Z). \quad (26)$$

Note that for any j , $\bar{\phi}_j = \bar{\Phi}_j/\epsilon$. According to the above positions, (11)–(13) become

$$\frac{\partial^2 \bar{\Phi}}{\partial y^2} + \epsilon^2 \frac{\partial^2 \bar{\Phi}}{\partial Z^2} = 0, \quad (27)$$

$$\frac{\partial \bar{\Phi}}{\partial y} - \epsilon^2 \frac{d\bar{\eta}}{dZ} \frac{\partial \bar{\Phi}}{\partial Z} = 0, \quad y = \bar{\eta}, \quad (28)$$

$$\left(\frac{\partial \bar{\Phi}}{\partial y}\right)^2 + \epsilon^2 \left(\frac{\partial \bar{\Phi}}{\partial Z}\right)^2 - \epsilon^2 [1 + Z(1-r)] = \epsilon^2 \frac{2}{WeR}, \quad y = \bar{\eta}, \quad (29)$$

which, solved to the zeroth and first order, give

$$\bar{\Phi}_0 = \bar{\Phi}_0(Z) = \frac{2}{3} \frac{[1 + Z(1-r)]^{3/2}}{1-r}, \quad (30)$$

$$\bar{\Phi}_1 = \bar{\Phi}_1(Z) = 0. \quad (31)$$

Since the non-dimensional flow rate is equal to unity it follows that

$$\bar{\eta}_0(Z) = [1 + Z(1-r)]^{-1/2}. \quad (32)$$

The second-order problem is

$$\frac{\partial^2 \bar{\Phi}_2}{\partial y^2} + \frac{\partial^2 \bar{\Phi}_0}{\partial Z^2} = 0, \quad (33)$$

$$\frac{\partial \bar{\Phi}_2}{\partial y} - \frac{d\bar{\eta}_0}{dZ} \frac{\partial \bar{\Phi}_0}{\partial Z} = 0, \quad (34)$$

$$\left(\frac{\partial \bar{\Phi}_2}{\partial y}\right)^2 + 2 \frac{\partial \bar{\Phi}_0}{\partial Z} \frac{\partial \bar{\Phi}_2}{\partial Z} = \frac{2}{We} \frac{d^2 \bar{\eta}_0}{dZ^2}, \quad y = \bar{\eta}_0. \quad (35)$$

Equations (33)–(35) are similar to those obtained by Geer & Strikwerda (1983) in a cylindrical coordinate system, but, in the present case, they do not need to be solved numerically. In fact, from (33) it follows that

$$\bar{\Phi}_2(y, Z) = -\frac{1}{4}y^2(1-r)[1 + (1-r)Z]^{-1/2} + C_1(Z)y + C_2(Z) \quad (36)$$

and $C_1(Z)$ and $C_2(Z)$ can be derived from (34) and (35). It follows that the basic flow potential, to within terms of $O(\epsilon^2)$, is

$$\begin{aligned} \bar{\Phi}(y, Z) &= \frac{2}{3} \frac{[1 + Z(1-r)]^{3/2}}{1-r} + \epsilon^2(1-r) \\ &\times \left[-\frac{1}{4}y^2[1 + Z(1-r)]^{-1/2} + \frac{1}{6}[1 + Z(1-r)]^{-3/2} - \frac{3}{8We}[1 + Z(1-r)]^{-2} + \tilde{\phi} \right] + O(\epsilon^4), \quad (37) \end{aligned}$$

where $\tilde{\phi}$ is an integration constant.

2.2. Disturbance equations

By substituting the perturbation quantities defined by (19)–(21), together with the solution for the main flow obtained above in (14)–(18), and equating coefficients of like powers of ϵ , the zeroth- and first-order problems are derived:

order ϵ^0 :

$$\frac{\partial^2 \phi_0}{\partial y^2} - (\alpha^2 + \beta^2) \phi_0 = 0, \quad (38)$$

$$\frac{\partial^2 \psi_0}{\partial y^2} - (\alpha^2 + \beta^2) \psi_0 = 0, \quad (39)$$

$$-i\omega\eta_0 - i\alpha\eta_0 \frac{\partial \bar{\Phi}_0}{\partial Z} + \frac{\partial \phi_0}{\partial y} = 0, \quad y = \bar{\eta}_0, \quad (40)$$

$$-i\omega\eta_0 + \frac{\partial \psi_0}{\partial y} = 0, \quad y = \bar{\eta}_0, \quad (41)$$

$$i\omega\phi_0 + i\alpha\phi_0 \frac{\partial \bar{\Phi}_0}{\partial Z} - i r \omega \psi_0 + \frac{(\alpha^2 + \beta^2)}{We} \eta_0 = 0, \quad y = \bar{\eta}_0; \quad (42)$$

order ϵ :

$$\frac{\partial^2 \phi_1}{\partial y^2} - (\alpha^2 + \beta^2) \phi_1 = -i \left(2\alpha \frac{\partial \phi_0}{\partial Z} + \frac{\partial \alpha}{\partial Z} \phi_0 \right), \quad (43)$$

$$\frac{\partial^2 \psi_1}{\partial y^2} - (\alpha^2 + \beta^2) \psi_1 = -i \left(2\alpha \frac{\partial \psi_0}{\partial Z} + \frac{\partial \alpha}{\partial Z} \psi_0 \right), \quad (44)$$

$$-i\omega\eta_1 - i\alpha\eta_1 \frac{\partial \bar{\Phi}_0}{\partial Z} + \frac{\partial \phi_1}{\partial y} = \eta_0 \frac{\partial \bar{\Phi}_0}{\partial Z} \frac{\partial \bar{\eta}_0}{\partial Z} + i\alpha\phi_0 \frac{\partial \bar{\eta}_0}{\partial Z} + \frac{\partial \bar{\Phi}_0}{\partial Z} \frac{\partial \eta_0}{\partial Z} - \eta_0 \frac{\partial^2 \bar{\Phi}_2}{\partial y^2}, \quad y = \bar{\eta}_0, \quad (45)$$

$$-i\omega\eta_1 + \frac{\partial \psi_1}{\partial y} = i\alpha\psi_0 \frac{\partial \bar{\eta}_0}{\partial Z}, \quad y = \bar{\eta}_0, \quad (46)$$

$$i\omega\phi_1 - i r \omega \psi_1 + i\alpha\phi_1 \frac{\partial \bar{\Phi}_0}{\partial Z} + \frac{\alpha^2 + \beta^2}{We} \eta_1 = -\frac{\partial \phi_0}{\partial y} \frac{\partial \bar{\Phi}_2}{\partial y} - \frac{\partial \phi_0}{\partial Z} \frac{\partial \bar{\Phi}_0}{\partial Z} + \frac{i}{We} \left(2\alpha \frac{\partial \eta_0}{\partial Z} + \eta_0 \frac{\partial \alpha}{\partial Z} \right), \quad y = \bar{\eta}_0, \quad (47)$$

where α is the wavenumber along Z , defined as

$$\alpha(Z) = \frac{\partial}{\partial Z} \gamma(Z). \quad (48)$$

Additional conditions expressing the symmetric or antisymmetric nature of the disturbance in the liquid and the asymptotic vanishing (for large y) of the disturbance in the gas have to be added.

The equations of the zeroth-order problem are formally identical to the ones obtained by considering a parallel mean flow, namely a sheet of constant thickness, although in this last situation the disturbance amplitude and wavenumber in the z -direction are independent of z . On the other hand, within the present approach the introduction of the slow scale Z and the WKB approximation allow one to account for the basic flow variation and to use a more general form of the disturbance (local formulation). The general integral for $\phi_0(y, Z)$ is

$$\phi_0(y, Z) = A(Z) \cosh [(\alpha^2 + \beta^2)^{1/2} y] + B(Z) \sinh [(\alpha^2 + \beta^2)^{1/2} y], \quad (49)$$

while the solution for $\psi_0(y, Z)$, since it has to vanish at large distances y from the interface, conveniently assumes the form

$$\psi_0(y, Z) = C(Z) [\cosh((\alpha^2 + \beta^2)^{1/2} y) - \sinh((\alpha^2 + \beta^2)^{1/2} y)]. \quad (50)$$

Since the governing differential system is linear and homogeneous, the even and odd solutions for ϕ_0 can be considered separately. Note that, physically, the odd solution corresponds to antisymmetric disturbances which displace each of the free surfaces in the same direction, giving rise to the so-called sinuous waves. On the other hand, the even solution corresponds to symmetric disturbances which displace the two interfaces in opposite directions giving rise to varicose waves. Accordingly, for the sinuous mode it follows that

$$\phi_{0s}(y, Z) = B(Z) \sinh((\alpha^2 + \beta^2)^{1/2} y). \quad (51)$$

Substitution of ϕ_{0s} and of (50) in (40)–(42) leads to an algebraic system of equations for which the existence of non-trivial solutions requires that

$$(\omega - \alpha \bar{w}_0)^2 \tanh((\alpha^2 + \beta^2)^{1/2} \bar{\eta}_0) + \omega^2 r - \frac{(\alpha^2 + \beta^2)^{3/2}}{We} = 0, \quad (52)$$

where the vertical velocity component $\bar{w}_0 = -\partial \bar{\Phi}_0 / \partial Z$ has been introduced.

The solution for the varicose mode is

$$\phi_{0v}(y, Z) = A(Z) \cosh((\alpha^2 + \beta^2)^{1/2} y) \quad (53)$$

and the corresponding stability characteristic equation is

$$(\omega - \alpha \bar{w}_0)^2 \coth((\alpha^2 + \beta^2)^{1/2} \bar{\eta}_0) + \omega^2 r - \frac{(\alpha^2 + \beta^2)^{3/2}}{We} = 0. \quad (54)$$

Equations (52) and (54) are generally referred to as dispersion relations.

The functions $A(Z)$ or $B(Z)$, $C(Z)$ and $\eta_0(Z)$ are still unknown to this level of approximation. Within the context of the present paper they may be assumed constant. In this sense the analysis developed here should be considered not properly non-parallel, but quasi-parallel. The actual functional dependence on Z can be determined to the first-order approximation, from the solvability condition for the inhomogeneous problem (43)–(47). However, this is outside the scope of the present work. Furthermore, to compare the results of the present analysis with those in the literature, where two-dimensional disturbances only are considered, the assumption $\beta = 0$ will be made in the following.

The dispersion relations (52) and (54) may be re-written respectively as

$$(\omega - \alpha)^2 \tanh \xi + \omega^2 r - \frac{\xi^3}{We_\eta} = 0 \quad (55)$$

$$\text{and} \quad (\omega - \alpha)^2 \coth \xi + \omega^2 r - \frac{\xi^3}{We_\eta} = 0, \quad (56)$$

where $\xi = (\alpha^2)^{1/2}$ and the non-dimensional frequency, wavenumber and Weber number are re-defined as

$$\omega = \frac{\omega^* \bar{\eta}_0^*}{\bar{w}_0^*}, \quad \alpha = \alpha^* \bar{\eta}_0^*, \quad We_\eta = \frac{\rho_l \bar{w}_0^{*2} \bar{\eta}_0^*}{\sigma}.$$

As usual, asterisks denote dimensional quantities and We_η is the local Weber number referred to the local velocity and sheet thickness.

Equations (55) and (56) coincide formally with those obtained by Squire (1953) except for the local character mentioned above. In the following they will be sometimes referred to as $D(\alpha, \omega) = 0$.

2.3. Stability analysis

As pointed out in the Introduction, the actual physical nature of solutions of the dispersion relation for complex wavenumbers can be determined by studying the asymptotic behaviour of a localized perturbation to the basic flow, introduced at a certain instant of time in a limited region or at just one point (i.e. by solving the initial value problem). The approach introduced by Clemmow & Dougherty (1969) in the context of plasma physics is employed in the present paper as a powerful tool to study the impulse response of the system and to diagnose the nature of the instability. Following closely Clemmow & Dougherty (1969) (to which the interested reader is referred for a complete development and explanation of the method), let the system response to the localized perturbation be represented by assuming the following form for the wave packet:

$$P(Z, t) = \int_{-\infty}^{+\infty} f(\omega) e^{i\alpha(\omega)Z} e^{-i\omega t} d\omega, \quad (57)$$

where $\alpha(\omega)$ is given by the dispersion relation and ω is considered a real variable. The function $f(\omega)$ determines the amplitude and phase of each locally plane wave component, and is assumed to decay as ω tends to infinity. It is crucial to stress the importance of the real coefficients in (55)–(56) and that $\alpha(\omega)$ is a multi-valued function, one branch of which has been considered in (57). Since $P(Z, t) \rightarrow 0$ as $t \rightarrow \pm\infty$ (Riemann–Lebesgue lemma), the disturbance is localized in time at any point in space. If it is also localized in space at any given time, it is a pulse which grows as it travels, that is an amplifying wave. Otherwise ‘the packet is not an acceptable physical idealization’ and the complex wavenumbers $\alpha(\omega)$ correspond to evanescent waves.

An alternative way to construct the wave-packet solution is

$$Q(Z, t) = \int_{-\infty}^{+\infty} g(\alpha) e^{i\alpha Z} e^{-i\omega(\alpha)t} d\alpha, \quad (58)$$

which is localized in space at every point in time. If it is also localized in time at every point in space, it is a pulse travelling as it grows, hence a convectively unstable perturbation. Otherwise the instability is absolute.

As Clemmow & Dougherty (1969) pointed out, a way to establish whether $P(Z, t)$ is also localized in space, or $Q(Z, t)$ localized in time, consists of trying to evaluate the integrals in (57) and (58) by interchanging the roles of α and ω . If this can be done, P and Q are equal for every Z and t and they are both localized. If in (57) the real ω -axis can be distorted in the complex ω -plane into a line which is map of the real α -axis, then

$$\lim_{Z \rightarrow \infty} P(Z, t) = 0 \quad (59)$$

and hence there is travelling wave amplification. In a similar way, referring to (58), if the real α -axis can be distorted in the complex α -plane into a line which is map of the real ω -axis then

$$\lim_{t \rightarrow \infty} Q(Z, t) = 0 \quad (60)$$

and the instability is clearly convected. Note explicitly that the limits in (59) and (60) represent the localization of the packet in space and time, respectively, thus both correspond to convective instability. On the other hand the definition of convective instability given by Briggs (1964) and Bers (1975) is recovered by (60), i.e. the

impulse response tends to vanish for all Z as $t \rightarrow \infty$. If Q is not localized in time $\lim_{t \rightarrow \infty} Q(Z, t) = \infty$, and this is the definition of absolute instability of Briggs (1964) and Bers (1975).

Convective instability and travelling wave amplification are different ways to describe the same phenomenon, and whether a system is convectively or absolutely unstable can be discovered by studying the mapping topology of $\alpha = \alpha(\omega)$. The situation in which real values only of both ω and α are found as solution of the dispersion relation corresponds to the case of a stable system. If, instead, ω is real for every real α , but complex α are found for a certain ω range, $\omega_1 < \omega < \omega_2$, the real ω -axis in the complex ω -plane cannot be deformed into a map of the real α -axis, since the gap between ω_1 and ω_2 cannot be bridged with any path along which α is real. The α and ω roles cannot be reversed in (57), the limit (59) does not hold, and the perturbations with complex α are evanescent waves. Conversely, when α is real for every real ω , but complex ω are found for some real $\alpha_1 < \alpha < \alpha_2$, the real ω -axis can be distorted in a line on which α is real but not vice versa. The α and ω roles cannot be reversed in (58), the limit (60) does not hold, and the instability arising for complex ω is absolute. Finally, consider the case in which complex ω are found for some real α and complex α are found for some real ω . This implies that the real ω -axis can be deformed into a line which is a map of the real α -axis in the complex ω -plane and vice versa for the real α -axis. The two limits (59) and (60) are both valid. Therefore the system is convectively unstable and the complex wavenumbers are really amplifying waves.

3. Results and discussion

The dispersion relations (55) and (56) are solved by means of a complex Newton method to obtain α as a function of ω . In order to apply the method of Clemmow & Dougherty (1969) the real values of α are plotted against the real values of ω for different values of the Weber number and the gas-to-liquid density ratio r . The relevant topology is analysed. If needed, the analysis of Briggs (1964) and Bers (1975) is also considered.

3.1. Sinuous modes

First, the particular case of $r = 0$ (absence of external gas) is examined, for which the imaginary part of the frequency ω_i vanishes for real α at any We_η . The α - ω plots corresponding to two typical local Weber numbers equal to 2 and 0.5 are shown in figures 2(a) and 2(b), respectively. In both plots ω is real for any real α , but complex α roots are found for some real ω . According to the discussion of §2.3 the flow should be defined as stable. However, as will be discussed later in detail for the case $r \neq 0$, one needs to verify if it is possible to extend the region of absolute convergence of the flow Green's function into the lower-half ω -plane (e.g. Bers 1975). In other words the highest pinch-type singularity $\omega_0 = \omega(\alpha_0)$ dominating the time-asymptotic behaviour of the Green's function has to be determined together with the order of this singularity. For the range $We_\eta < 1$ the highest pinch-type singularity occurs (not shown here) at complex $\alpha_0 = 0$ (corresponding to complex $\omega_0 = 0$), and in the neighbourhood of the point α_0, ω_0 the dispersion relation behaves as $(\omega - \omega_0)^2 \approx (\alpha - \alpha_0)^2$. This is in agreement with a result of Lin *et al.* (1990) following which the Green's function remains bounded but non-vanishing for all time and any finite Z . Lin *et al.* (1990) termed this occurrence *pseudo-absolute instability* because the entire flow field remains perturbed.

On the other hand, for the range $We_\eta > 1$ it is found that two pinch-points occur at real $\pm \alpha_0$ ($\alpha_0 \neq 0$ and depending on We_η) and real ω_0 ($\omega_0 \neq 0$). Near these singularities

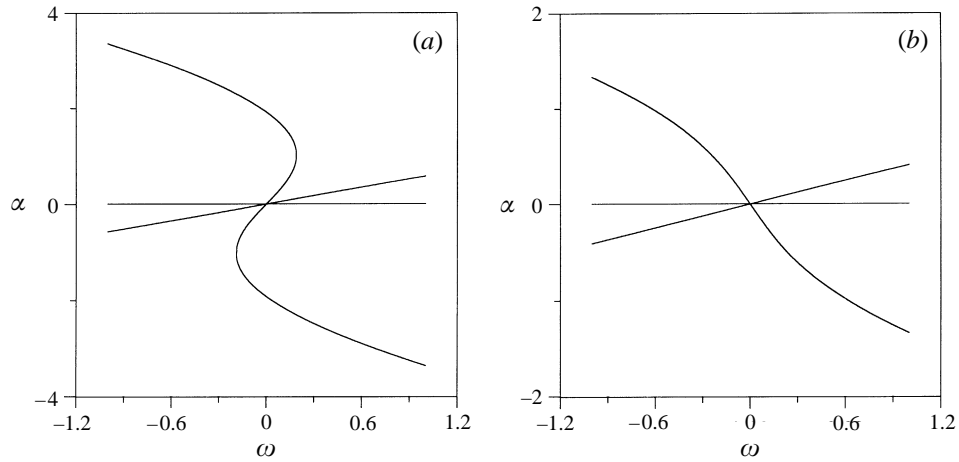


FIGURE 2. Sinuous modes: real roots of the dispersion relation in the absence of ambient gas. (a) $We_\eta = 2$, (b) $We_\eta = 0.5$.

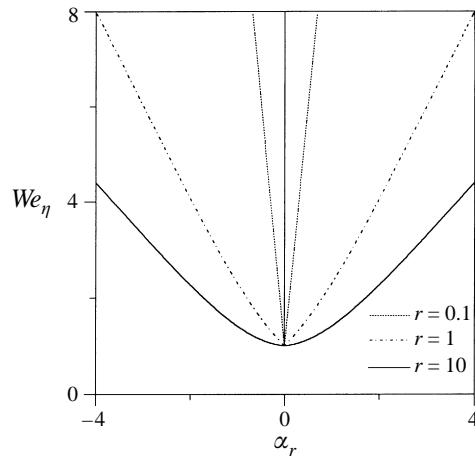


FIGURE 3. Neutral stability curve for sinuous disturbances and various gas-to-liquid density ratios.

the dispersion relation behaves as $(\omega - \omega_0) \approx (\alpha - \alpha_0)^2$, hence the relevant Green's function G is such that

$$\lim_{t \rightarrow \infty} G(Z, t) \approx t^{-1/2} \quad (61)$$

for all Z . Therefore the sheet is stable.

Note that Lin (1981), who employed a spatial modes approach, stated the sheet to be temporally stable, but spatially unstable for $We_\eta < 1$, namely for disturbances whose group velocity is directed upstream.

Consider now the case of r different from zero where, according to Squire (1953), instability arises when We_η is (locally) greater than unity. This can be immediately seen by examining the neutral stability curve, i.e. the locus of $\omega_i = 0$ in the (α_r, We_η) -plane, which is defined by

$$We_\eta = \frac{\xi \tanh \xi + r}{r \tanh \xi} \quad (62)$$

and is plotted in figure 3 for various values of the gas-to-liquid density ratio r . In the

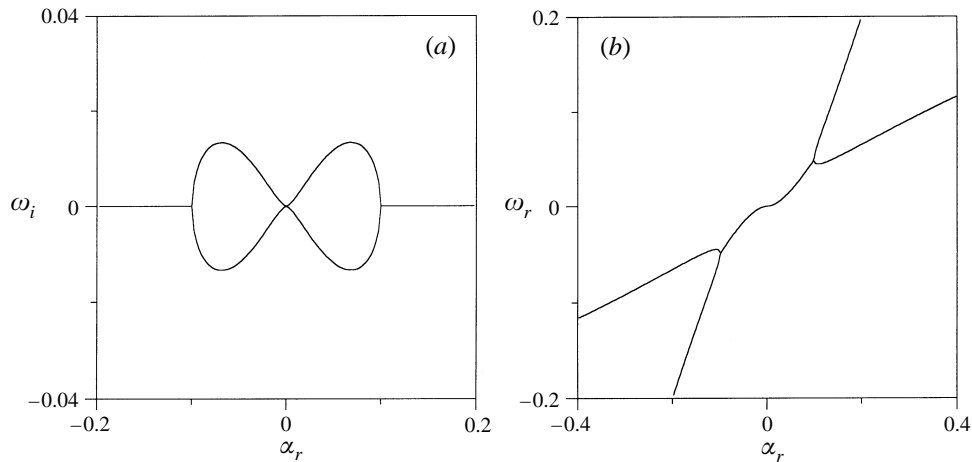


FIGURE 4. (a) Imaginary part and (b) real part of the ω eigenvalues as a function of the real wavenumber. $r = 0.1$, $We_\eta = 2$.

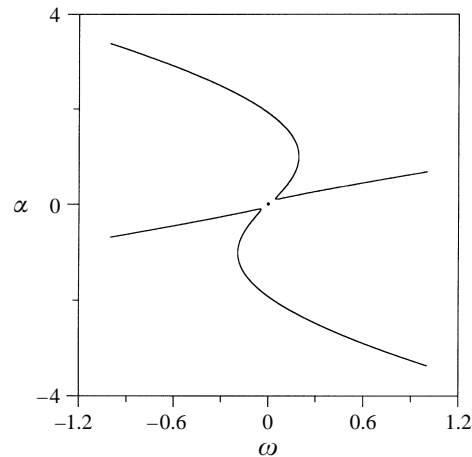
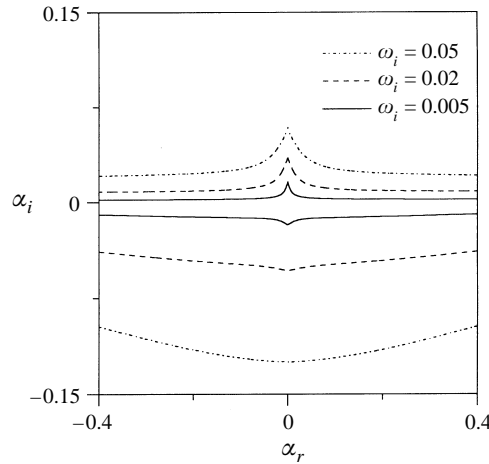


FIGURE 5. Local convective instability of sinuous modes. $r = 0.1$, $We_\eta = 2$.

range $We_\eta > 1$ for any given We_η and r there exists a limited band of real wavenumbers for which $\omega_i > 0$, while outside this interval, as well as in the whole region below $We_\eta = 1$, $\omega_i = 0$. Figure 4(a) shows the ω_i trend for a typical case in the range $We_\eta > 1$, namely $We_\eta = 2$ and $r = 0.1$, while figure 4(b) depicts ω_r as a function of α_r . From figure 3 note also that the vertical axis $\alpha_r = 0$ does not belong to the region of instability whose lower bound, namely $We_\eta = 1$, is independent of the gas-to-liquid density ratio. Moreover, all along the neutral stability curve the dispersion relation admits double real roots of ω for any given real α . In particular at $\alpha_r = 0$, $\omega_r = 0$ also.

The α - ω topology for the same case as figure 4 is shown in figure 5. Complex values of ω are present for a range of real α across zero, and complex α are conversely found for a range of real ω . Note that the real point $\alpha_r = \omega_r = 0$ is an isolated root of the dispersion relation, as already noted. According to the discussion in §2.3 concerned with the analysis of Clemmow & Dougherty (1969), the system supports local convective instabilities and the complex values of α represent waves which grow as they travel. The flow in its time-asymptotic state behaves as an amplifier of external disturbances, i.e. following Monkewitz (1990) it is globally stable (no self-sustained


 FIGURE 6. Pinch-type singularity in the complex α -plane. $r = 0.1$, $We_\eta = 0.5$.

resonant states may arise) if boundary and long-range feedback effects are absent or negligible. This finding matches the situation described heuristically by Brown (1961) who pointed out that if the momentum flux is greater than 2σ a hole appearing in the curtain ‘does not grow but will be carried out away with the curtain’. Actually the sheet is locally convectively unstable due to the presence of the ambient gas. The flow receptivity to input frequencies should be analysed by solving the relevant signalling problem.

Consider now the case of $We_\eta < 1$ where $\omega_i = 0$ for any real α (see figure 3). The system cannot be defined stable because again it is necessary to verify if it is possible to extend the region of absolute convergence of the flow Green’s function into the lower-half ω -plane. For the present situation this is not the case because the highest pinch-type singularity α_0, ω_0 such that $D(\alpha_0, \omega_0) = 0$ and $(\partial D / \partial \alpha)_{\alpha_0, \omega_0} = 0$, dominating the asymptotic behaviour in time of the Green’s function, occurs just at the complex point $\alpha_0 = 0$. Here the dispersion relation (55), in this connection referred to briefly as $D(\alpha, \omega) = 0$, gives the complex $\omega_0 = 0$. This is shown in a standard way, see Briggs (1964) and Bers (1975), in figure 6 referred to the complex α -plane where the relevant $\alpha(\omega)$ branches pertaining to the singularity originate from distinct upper and lower halves of the α -plane as ω_i is decreased from positive values towards zero. It should be noted that the upper and lower branches both tend to coincide with the real axis $\alpha_i = 0$, but the pinch is located at $\alpha_r = \alpha_i = 0$ (where $\omega_r = 0$ also) because for any given ω_i , as ω_r is increased, the upper curve is generated from left to right, whilst the lower one is from right to left.

To determine the actual time-asymptotic behaviour of the Green’s function, the analytic form of the dispersion relation (55) in the vicinity of the pinch singularity $\alpha_0 = \omega_0 = 0$ may be approximate by means of an expansion in a Taylor series. In addition to $D(0, 0) = (\partial D / \partial \alpha)_{0,0} = 0$, it is also found

$$(\partial^2 D / \partial \alpha^2)_{0,0} = (\partial D / \partial \omega)_{0,0} = (\partial^2 D / \partial \alpha \partial \omega)_{0,0} = 0$$

so that in the neighbourhood of the singularity $(\omega - \omega_0)^2 \approx (\alpha - \alpha_0)^3$. Following once again Bers (1975), the Green’s function grows at a time rate which is given by

$$\lim_{t \rightarrow \infty} G(Z, t) \approx \lim_{t \rightarrow \infty} \int_{\omega_0} \frac{e^{i\alpha_0 Z}}{(\omega - \omega_0)^{4/3}} e^{-i\omega t} \frac{d\omega}{2\pi}, \quad (63)$$

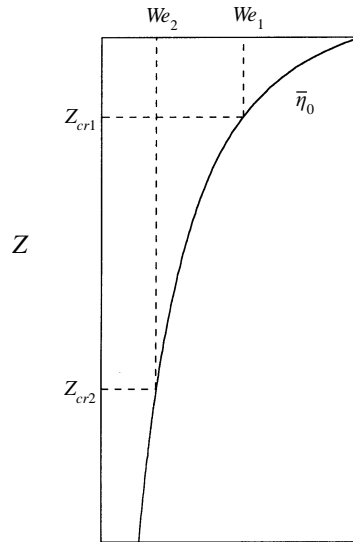


FIGURE 7. Location of transition from absolute to convective instability along the sheet.

hence

$$\lim_{t \rightarrow \infty} G(Z, t) \approx t^{1/3} \quad (64)$$

for all Z . The time-asymptotic response grows *algebraically* in time at all locations in space, thus an absolute instability is found for $We_\eta < 1$. Note that the factor $t^{1/3}$ arises from the interference of components of the packet and is strictly connected with the analytic form of the dispersion relation in the vicinity of the pinch-type singularity.

This conclusion deserves further discussion because on the one hand it seems to agree with Brown's (1961) statement, that 'if the momentum flux is less than 2σ a hole in the curtain will grow and disrupt the curtain', but on the other hand it does not agree with other findings of Lin *et al.* (1990). They developed a viscous analysis and detected a pinch-type singularity located at $\alpha_0 = \omega_0 = 0$. On the grounds of the order of this singularity, they found that disturbances are bounded but non-vanishing. As for the case $r = 0$ they proposed calling this situation *pseudo-absolute instability*. Indeed, the different time-asymptotic behaviour of the Green's function found by Lin *et al.* (1990) is strictly linked to the presence of the viscosity, as will be discussed later in this section.

A major result of the present paper is that the system behaves locally in two different ways depending on the local Weber number: the sheet is absolutely unstable (with algebraic growth of disturbances) where $We_\eta < 1$, and it is convectively unstable where $We_\eta > 1$. By introducing the liquid flow rate per unit length $Q = 2\bar{U}b$ the flow Weber number, (6), may be re-written as $We = \rho_l Q^2 / (4\sigma b)$. The condition for convective instability, stated above as $We_\eta > 1$, turns out to be $\bar{\eta}_0 < We$. It is easy to see that the vertical location Z_{cr} at which the sheet starts to become convectively unstable moves downstream as the liquid flow rate is reduced or the surface tension is increased. This is shown in figure 7 where a typical trend of the sheet thickness as a function of the vertical spatial coordinate Z is reported. It is clear that if $We_2 < We_1$, then $Z_{cr2} > Z_{cr1}$, in agreement with the experimental observation of Crapper *et al.* (1973).

In summary in this paper a transition from absolute to convective local instability is proposed that occurs where the flow Weber number equals the dimensionless sheet thickness. To relate the local stability properties to the global behaviour of the sheet consider that, as first pointed out by Chomaz *et al.* (1988) and further established by

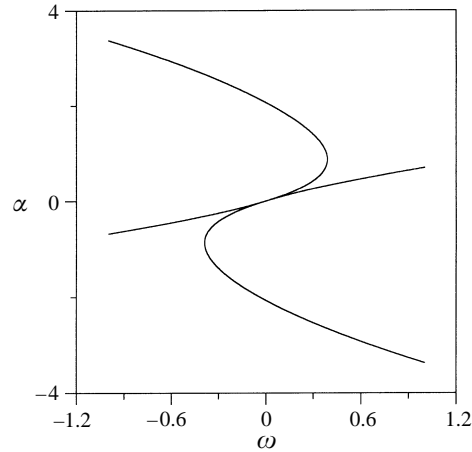


FIGURE 8. Varicose modes. Real roots of the dispersion relation in the absence of ambient gas. $We_\eta = 2$.

Monkewitz (1990), the local absolute instability may lead to a global instability. In other words, the existence of a region of absolute instability is a necessary but not sufficient condition for the onset of amplified global oscillations. The region of absolute instability must reach a critical size in order for resonances to occur. As proved by Chomaz *et al.* (1988) for a Ginzburg–Landau model, the receptivity of the flow to input frequencies, i.e. for the present situation the enforcement of the boundary conditions at the nozzle exit, increases as the region of absolute instability becomes longer. This last finding resembles an analogous result obtained by Monkewitz (1990) for the onset of dripping in a round capillary jet. It agrees also with the experimental evidence (de Luca & Meola 1995) that the two-dimensional sheet breaks up as the flow rate is reduced, all other quantities being kept constant.

The algebraic growth found for $We_\eta < 1$ is strictly linked to the order of the singularity dominating the time behaviour of the Green's function, and hence to the occurrence of double real- ω eigenvalues. The role of the algebraic growth was recently discussed by Trefethen *et al.* (1993) within the so-called method of pseudospectra. In that paper it is shown that if the operator of the linearized problem is far from normal the eigenvalues determine correctly the long-time behaviour, not the transient. Generally the transient growth of flow perturbations, i.e. the short-time system response, is inviscid and is eventually followed by viscous decay (if linearity is preserved up to that stage) due to the splitting of the roots. Hence, it may be conjectured that if viscosity is added to the present model it acts to reduce the order of the singularity dominating the (short-time) system response for $We_\eta < 1$, and to remove possibly the absolute instability. However, the time after which this effect occurs could be not sufficient to avoid nonlinear growth leading to the actual sheet break-up. It has to be remembered that Crapper *et al.* (1975*b*) also demonstrated that viscosity has no effect on the initial stages of wave growth on the sheet. The question is that the two-dimensional liquid sheet is presumably one of those systems where the crucial phenomena are of short-time nature.

3.2. Varicose modes

When varicose modes are considered, no difference is found between the α - ω topologies obtained for Weber numbers less or greater than unity. Figure 8 shows that in the absence of external gas ($r = 0$) no $\omega_i > 0$ are found for any real α and no *pseudo-*

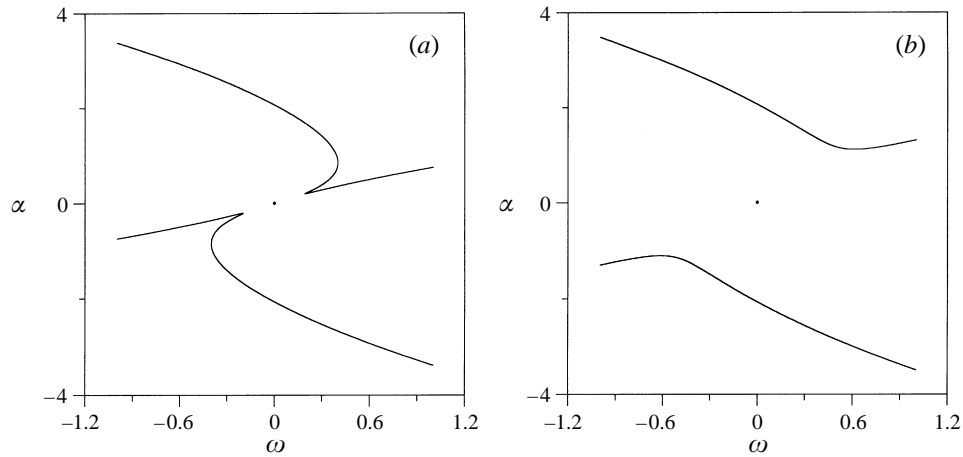


FIGURE 9. Local convective instability of varicose modes. $We_\eta = 2$: (a) $r = 0.1$, (b) $r = 1$.

absolute instability occurs. Hence the sheet is stable. Convective instabilities arise for gas-to-liquid density ratios different from zero. Like the sinuous modes, the instability range gets larger with increasing r , as is evident from figure 9. This confirms the result of Lin *et al.* (1990) stating that the convective instability of varicose waves depends on the external gas as well.

4. Conclusions

The linear stability of an inviscid two-dimensional liquid sheet falling vertically under gravity has been studied by analysing the asymptotic behaviour of a disturbance added to the system at a certain instant of time, that is to say the wave-packet solution to the initial-value problem. Contrary to all the previous papers the effect of gravity is fully taken into account. This breaks the Galilean invariance along the streamwise direction, namely the flow in its unperturbed state is spatially developing. However, since for slender sheets the evolution length scale is larger than the sheet thickness, a slow length scale has been introduced, so as to consider the flow as slightly non-parallel.

The flow stability properties that have been established referred to local velocity and certain thickness. Indeed, the dispersion relations obtained for both sinuous and varicose disturbances coincide with those already found by Squire (1953), but they exhibit the local character mentioned above and involve the local Weber number We_η .

Following CLEMMOW & DOUGHERTY (1969) the nature of instability of the liquid sheet has been studied basically by analysing the mapping topology in the (α, ω) -plane. If needed, the method of BRIGGS (1964) and BERS (1975) has been also applied. The local stability properties have been related to the global behaviour of the flow by following the analysis developed by CHOMAZ *et al.* (1988) and MONKEWITZ (1990).

For sinuous disturbances in the presence of external gas a critical local We_η equal to unity has been found, below which the sheet is absolutely unstable (with algebraic growth of disturbances) and above which it is convectively unstable. This confirms that the critical Weber number is insensitive to the viscosity and the gas-to-liquid density ratio.

The critical distance of transition from absolute to convective local instability, as

measured from the nozzle exit section, increases with decreasing the flow Weber number (namely, for instance, the liquid flow rate per unit length), but is independent of the gas-to-liquid density ratio. It is hypothesized that the sheet behaves as a globally unstable system (in the sense that it is unstable to global infinitesimal fluctuations in the entire flow field) only if the region of absolute instability is sufficiently long. This finding agrees with the experimental evidence that the sheet breaks up as the flow rate is reduced, all other quantities being kept constant. Although it is believed that viscosity may act to remove the (absolute) algebraic growth of disturbances, the time after which this occurs could not be sufficient to avoid possible nonlinear phenomena appearing and breaking up the sheet. The development of a stability analysis based on the pseudospectra theory, with a viscous model and three-dimensional perturbations, is strongly recommended. The connection between local and global stability properties also needs to be studied quantitatively.

For varicose modes convective instabilities arise at any Weber number and gas-to-liquid density ratios different from zero. In both the sinuous and the varicose cases the unstable wavenumbers range gets larger with increasing r .

REFERENCES

- BERS, A. 1975 Linear waves and instabilities. In *Physique des Plasmas* (ed. C. De Witt & J. Peyraud). Gordon & Breach.
- BRIGGS, R. J. 1964 *Electron-Stream Interaction with Plasmas*. The MIT Press.
- BROWN, D. R. 1961 A study of the behaviour of a thin sheet of a moving liquid. *J. Fluid Mech.* **10**, 297–305.
- CHOMAZ, J. M., HUERRE, P. & REDEKOPP, L. G. 1988 Bifurcations to local and global modes in spatially developing flows. *Phys. Rev. Lett.* **60**, 25–28.
- CHUBB, D. L., CALFO, F. D., MCCONLEY, M. W., MCMASTER, M. S. & AFJEH, A. A. 1994 Geometry of thin liquid sheet flows. *AIAA J.* **32**, 1325–1328.
- CLEMMOW, P. C. & DOUGHERTY, J. P. 1969 *Electrodynamics of Particles and Plasmas*. Addison-Wesley.
- CRAPPER, G. D., DOMBROWSKI, N., JEPSON, W. P. & PYOTT, A. D. 1973 A note on the growth of Kelvin–Helmholtz waves on thin liquid sheets. *J. Fluid Mech.* **57**, 671–672.
- CRAPPER, G. D., DOMBROWSKI, N. & PYOTT, A. D. 1975*a* Large amplitude Kelvin–Helmholtz waves on thin liquid sheets. *Proc. R. Soc. Lond. A* **342**, 209–224.
- CRAPPER, G. D., DOMBROWSKI, N. & JEPSON, W. P. 1975*b* Wave growth on thin sheets of non-Newtonian liquids. *Proc. R. Soc. Lond. A* **342**, 225–236.
- DRAZIN, P. G. & REID, W. H. 1981 *Hydrodynamic Stability*. Cambridge University Press.
- FINNICUM, D. S., WEINSTEIN, S. J. & RUSCHAK, K. J. 1993 The effect of applied pressure on the shape of a two-dimensional liquid curtain falling under the influence of gravity. *J. Fluid Mech.* **255**, 647–665.
- GEER, J. F. 1977 Streams with gravity: outer asymptotic expansion I. *Phys. Fluids* **20**, 1613–1621.
- GEER, J. F. & STRIKWERDA, J. C. 1983 Vertical slender jets with surface tension. *J. Fluid Mech.* **135**, 155–169.
- HAGERTY, W. W. & SHEA, J. F. 1955 A study of the stability of plane fluid sheets. *Trans. ASME E: J. Appl. Mech.* **22**, 509–514.
- HUERRE, P. & MONKEWITZ, P. A. 1990 Local and global instabilities in spatially developing flows. *Ann. Rev. Fluid Mech.* **22**, 473–537.
- LI, X. & TANKIN, R. S. 1991 On the temporal instability of a two-dimensional viscous liquid sheet. *J. Fluid Mech.* **226**, 425–443.
- LIN, S. P. 1981 Stability of a viscous liquid curtain. *J. Fluid Mech.* **104**, 111–118.
- LIN, S. P. & LIAN, Z. W. 1989 Absolute instability of a liquid jet in a gas. *Phys. Fluids A* **1**, 490–493.
- LIN, S. P., LIAN, Z. W. & CREIGHTON, B. J. 1990 Absolute and convective instability of a liquid sheet. *J. Fluid Mech.* **220**, 673–689.

- DE LUCA, L. & COSTA, M. 1995 Two-dimensional flow of a liquid sheet under gravity. *Computers Fluids* **24**, 401–414.
- DE LUCA, L. & MEOLA, C. 1995 Surfactant effects on the dynamics of a thin liquid sheet. *J. Fluid Mech.* **300**, 71–85.
- MONKEWITZ, P. A. 1990 The role of absolute and convective instability in predicting the behavior of fluid systems. *Eur. J. Mech. B/Fluids* **9**, 395–413.
- SQUIRE, H. B. 1953 Investigation of the instability of a moving liquid film. *Brit. J. Appl. Phys.* **4**, 167–169.
- TREFETHEN, L. N., TREFETHEN, A. E., REDDY, S. C. & DRISCOLL, T. A. 1993 Hydrodynamic stability without eigenvalues. *Science* **261**, 578–584.